研究成果の刊行に関する一覧表

| 発表者氏名 | 論文タイトル名 | 発表誌名 | 巻号 | ページ | 出版年 |
|---|---|---|---|---|---|
| Nakatani, K.; Horie, S.; Goto, Y.; Kobori, A.; Hagihara, S. | Evaluation of mismatch-binding ligands as inhibitors for Rev-RRE interaction | *Bioorg. Med. Chem.* | *14* | 5384-5388 | **2006** |
| Peng, T.; Dohno, C.; Nakatani, K. | Mismatch binding ligands function as molecular glue for DNA | *Angew. Chem. Int. Ed.* | *45* | 5623-5626 | **2006** |
| Hayashi, G.; Hagihara, M.; Kobori, A.; Nakatani, K. | Detection of L-DNA-Tagged PCR Products by Surface Plasmon Resonance Imaging | *ChemBio Chem* | *8* | 169-171 | **2007** |
| Peng, T.; Dohno, C.; Nakatani, K. | Bidirectional Control of Gold Nanoparticle Assembly by Turning On and Off DNA Hybridization with Thermally Degradable Molecular Glue | *ChemBio Chem* | *8* | 483-485 | **2007** |
| Takei, F.; Suda, H.; Hagihara, M.; Zhang, J.; Kobori, A.; Nakatani, K. | Allele Specific C-Bulge Probes with One Unique Fluorescent Molecule Discriminate the Single Nucleotide Polymorphism in DNA | *Chem. Eur. J.* | *in press* | | **2007** |
| Li, X.; Song, H.; Nakatani, K.; Kraatz, H.-B. | Exploiting Small Molecule Binding to DNA for the Detection of Single-Nucleotide Mismatches and Their | *Anal. Chem.* | *79* | 2552-2555 | **2007** |

| | | | | | |
|---|---|---|---|---|---|
| | Base Environment | | | | |
| Goto, Y.; Hagihara, S.; Hagihara, M.; Nakatani, K. | Small molecule binding to non-Quadruplex form of the Human Telomeric Sequence | *ChemBio Chem* | *in press* | | **2007** |
| Dohno, C.; Nakatani, K. | Control of DNA hybridization by photoswitchable mismatch binding ligands. | *Nucleic Acids Symp. Ser.* | *50* | 87-88 | **2006** |
| Hagihara, M.; Nakatani, K. | Inhibition of DNA replication by a d(CAG) repeat binding ligand | *Nucleic Acids Symp. Ser.* | *50* | 147-148 | **2006** |
| Tanaka, Y.; Yamaguchi, H.; Oda, S.; Kondo, Y.; Nomura, M.; Kojima, C.; Ono, A. | NMR spectroscopic study of a DNA duplex with mercury-mediated T-T basepairs | *Nucleosides Nucleotides Nucleic Acids* | *25* | 613-624 | **2006** |
| Furuita, K.; Mishima, M.; Kojima, C. | $^{1}H$, $^{13}C$ and $^{15}N$ resonance assignments of the VAP-A: OSBP complex | *J. Biomol. NMR* | *36 Suppl 5* | 69 | **2006** |
| Tanaka, Y.; Oda, S.; Yamaguchi, H.; Kudo, M.; Kondo, Y.; Kojima, C.; Ono, A. | Structural analyses on the mercury$^{II}$- mediated T-T base pair | *Nucleic Acids Symp. Ser.* | *50* | 47-48 | **2006** |
| Furuita, K.; Ishizaki, I.; | Studies of DNA recognition mechanism | *Nucleic Acids* | *50* | 259-261 | **2006** |

| | | | | | |
|---|---|---|---|---|---|
| Fukada, H.; Yamamoto, K.; Matsuyama, T.; Nomura, M.; Mishima, M.; Kojima, C. | of transcription factor IRF-4 | *Symp. Ser.* | | | |
| Tanaka, Y.; Oda, S.; Yamaguchi, H.; Kondo, Y.; Kojima, C.; Ono , A. | $^{15}N$-$^{15}N$ *J*-coupling across $Hg^{II}$: Direct observation of $Hg^{II}$-mediated T-T base pairs in a DNA duplex | *J. Am. Chem. Soc.* | *129* | 244-245 | **2007** |
| Mishima, M.; Wakabayashi, S.; Kojima, C. | Solution structure of the cytoplasmic region of $Na^+/H^+$ exchanger 1 complexed with essential cofactor calcineurin B homologous protein 1 | *J. Biol. Chem.* | *282* | 2741-2751 | **2007** |

研究成果の刊行物・別刷

Available online at www.sciencedirect.com
SCIENCE DIRECT
Bioorganic & Medicinal Chemistry
ELSEVIER
Bioorganic & Medicinal Chemistry 14 (2006) 5384–5388

# Evaluation of mismatch-binding ligands as inhibitors for Rev–RRE interaction

Kazuhiko Nakatani,[a,b,*] Souta Horie,[a] Yuki Goto,[a] Akio Kobori[a,†] and Shinya Hagihara[a,‡]

[a]*Department of Synthetic Chemistry and Biological Chemistry, Faculty of Engineering, Kyoto University, Kyoto 615-8510, Japan*
[b]*The Institute of Scientific and Industrial Research (SANKEN), Osaka University, 8-1 Mihogaoka, Ibaraki 567-0047, Japan*

Received 18 January 2006; revised 20 March 2006; accepted 21 March 2006
Available online 5 April 2006

**Abstract**—Drugs targeting the stem-loop IIB of Rev responsible element (RRE) of HIV-1 mRNA are potential therapeutic agents for HIV-1 infection. The stem loop is characterized by an internal loop consist of consecutive G-G and G-A mismatches, which is the single binding site for Rev protein for nuclear export of viral mRNA. We report here that ligands binding to G-G and G-A mismatches in duplex DNA also bind to the internal loop in competition with Rev peptide and lead to the dissociation of pre-formed Rev–RRE complex in a model system.


## 1. Introduction

The Rev responsible element (RRE) of HIV-1 mRNA is a large RNA structure residing within the region that codes envelope proteins[1] and serves as a docking site for the Rev protein.[2,3] Binding of the Rev protein to RRE induces the nuclear export to the cytoplasm of unspliced or partially spliced viral mRNA. Interference in the formation of the Rev–RRE complex inhibits nuclear transport of the unspliced mRNA, eventually causing suppression of HIV-1 replication. An internal loop in stem-loop IIB of RRE has been identified as a single high-affinity site for the Rev binding[4,5] (Chart 1). Thus, small molecular ligands that bind to the loop in competition with Rev protein are potential therapeutic agents for treating HIV-1 infection.[6–8]

However, the design of RNA targeting molecules still remained to be a challenge in medicinal chemistry because of the complicated RNA secondary and tertiary structures.[9–11] We have discovered a novel class of compounds that bind selectively to the mismatched base pair in duplex DNA. The stem-loop IIB of HIV-1 RRE is characterized by an internal loop consisting of two consecutive mismatched base pairs, one a G-G mismatch and the other a G-A mismatch. These non-Watson–Crick base pairs have been shown to be responsible for the Rev binding. We here report that naphthyridine dimer (**ND**)[12,13] and naphthyridine–azaquinolone (**NA**)[14,15] which bind to the G-G and G-A mismatches in duplex DNA, respectively, are the potential candidates of drug lead that inhibits the Rev–RRE interaction (Chart 2).

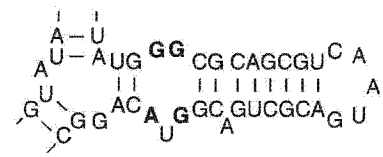

stem-loop IIB of HIV-1 RRE

**Chart 1.** A structure of stem-loop IIB of HIV-1 mRNA.

## 2. Results and discussion

We first qualitatively evaluated the binding of **ND** and **NA** to various RNA structures using surface plasmon resonance (SPR) assay with the sensors carrying **ND**

*Keywords*: RNA recognition; Inhibitors; Drug design; HIV-1 RRE.
* Corresponding author. Tel.: +81 6 6879 8455; fax: +81 6 6879 8459; e-mail: nakatani@sanken.osaka-u.ac.jp
† Present address: Department of Polymer Science and Engineering, Kyoto Institute of Technology, Matsugasaki, Sakyo-ku, Kyoto 606-8585, Japan.
‡ Present address: RIKEN (The Institute of Physical and Chemical Research), 2-1 Hirosawa, Wako-shi, Saitama 351-0198, Japan.

0968-0896/$ - see front matter © 2006 Elsevier Ltd. All rights reserved.
doi:10.1016/j.bmc.2006.03.038

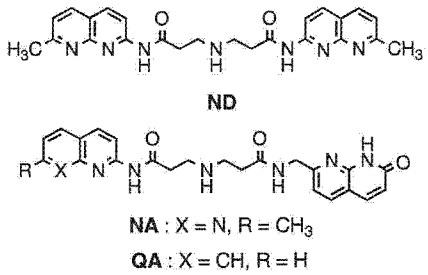


**Chart 2.** Structures of ligands used in these studies.

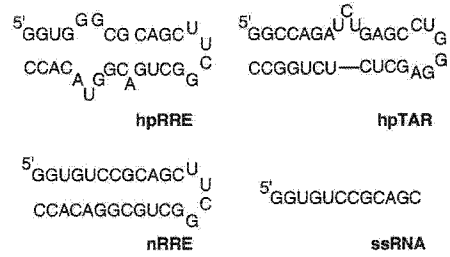


**Chart 4.** RNAs used in these studies and their possible secondary structures.

and **NA** on the surfaces. **ND** was immobilized as **aminolink-ND** at the secondary nitrogen by way of a short aminoalkyl linker onto the surface of carboxymethyl dextran of a CM5 sensor chip (BIAcore) (Chart 3).[12] **NA** was immobilized as a form of amino-linked dimer (**aminolink-NA**) to increase a surface density of the ligand,[15] because the **NA**-binding to a G-A mismatch in RNA was anticipated to be weaker than the **ND**-binding to a G-G mismatch based on their bindings to the mismatches in duplex DNA. Using the **ND**-immobilized sensor, a strong SPR response was observed for a hairpin RNA (**hpRRE**) (Chart 4) representing the stem-loop IIB of HIV-1 RRE (Fig. 1a). In contrast, a completely matched hairpin RNA (**nRRE**), which lacked an internal loop consisting of the G-G and G-A mismatches, did not bind to the **ND**-immobilized sensor surface. Very weak binding was observed for a single stranded RNA (**ssRNA**) and a hairpin RNA representing TAR RNA of HIV-1 (**hpTAR**) containing the r(UCU) bulge. SPR analyses with **NA**-immobilized surfaces showed a strong SPR response for **hpRRE**, whereas virtually no responses for other three RNAs (Fig. 1b). These experiments demonstrated that both **ND** and **NA** did not bind to a completely matched RNA duplex, r(UUCG) and r(CUGGGA) hairpin loops, and a r(UCU) bulge. Thus, the internal loop consisting of the G-G and G-A mismatches in **hpRRE** is most likely the binding site of both **ND** and **NA**.

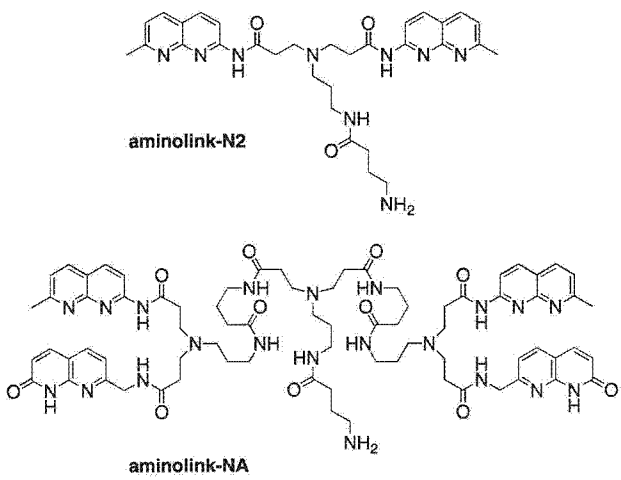


**Chart 3.** Structures of **aminolink-ND** and **aminolink-NA** used for the immobilization of **ND** and **NA**, respectively, onto the SPR sensor surface.

Separate experiments showed that **ND**-binding to the G-G mismatches in duplex RNA was favorable for those flanked by a single nucleotide bulge. (Table 1) The increase of $T_m$ ($\Delta T_m$) of G-G mismatch RNA duplex was 4.8 °C, whereas it increased up to 9.1 °C when the G-G mismatch was flanked by a single uridine and adenine bulge. Since the single uridine and adenine bulge in RNA duplex was not the site of the **ND** binding, it is most likely that structural perturbation on the G-G mismatch by the neighboring nucleotide bulge favorably affected the **ND**-binding to the G-G mismatch in RNA duplexes. The RNA duplex is known to have A-form, which has a deep major groove compared to that of B-form DNA duplex. **ND** binds to the G-G mismatch from the major groove side of DNA duplex. Thus, the single nucleotide bulge flanking the G-G mismatch may loosen the deep major groove to facilitate the **ND**-binding.

The binding of **ND** and **NA** to the stem-loop IIB of RRE was examined with respect to the structure of the heterocycles in the ligand. We measured the difference in the absorption spectra of ligands between the absence and presence of **hpRRE**. The absorption of unbound **ND** at 320 nm decreased with a concomitant bathochromic shift as indicated by an increased absorption at 345 nm (Fig. 2a). Similar changes in the UV spectra were observed for **NA** with a decreased efficiency. Bathochromic shifts of the ligand absorptions suggested the stacking interaction of bound **ND** and **NA** with the neighboring bases in **hpRRE**. In contrast, a ligand, aminoquinoline–azaquinolone (**QA**), which did not bind to the G-G and G-A mismatches in duplex DNA,[14] showed little absorption change in the spectra. A complete loss of binding as observed for **QA** suggested an important role of 2-aminonaphthyridine for the binding to **hpRRE**. The UV absorption change of these ligands in the presence of **nRRE** was quite small with virtually no bathochromic shift, strongly suggesting that the internal loop in **hpRRE** would be the site of binding of **ND** and **NA** (Fig. 2b).

Having the data indicating the binding of **ND** and **NA** to **hpRRE**, we investigated competitive binding of these molecules with the Rev model peptide 5,6TAMRA-TRQARRNRRRRWRERQRAAAAK-amide (**tamRev**) by fluorescence anisotropy displacement assay.[6,16] The peptide consisted of an arginine-rich motif ($Rev_{34-50}$) and an alanine-rich sequence, and was previously shown to interact with high affinity to RRE stem-loop IIB.[6,17]

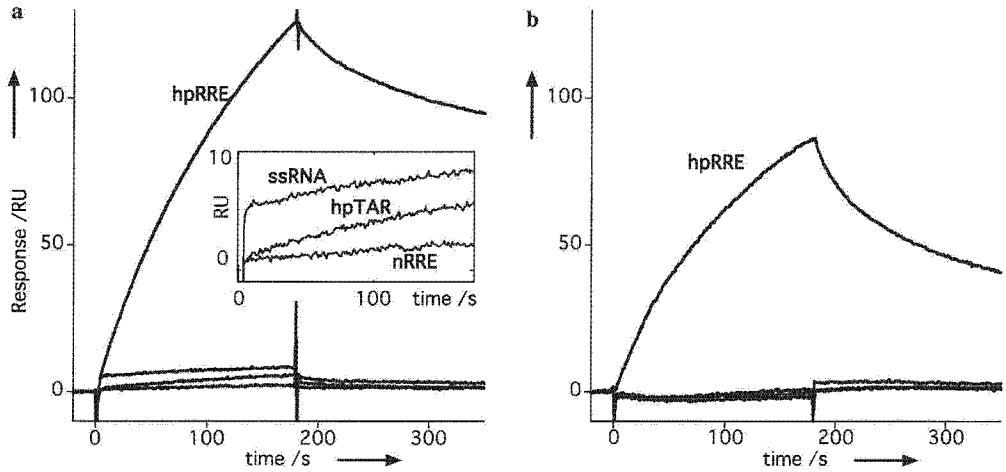


**Figure 1.** SPR assays of RNA-binding to the ligand-immobilized sensor surfaces. RNA sample (**hpRRE**, **nRRE**, **hpTAR**, and **ssRNA**, each 100 nM) in 10 mM HEPES and 150 mM NaCl was heat denatured, folded by slow cooling, and applied to the sensor for 180 s with a flow rate of 30 μL/min. (a) **ND**-immobilized sensor surface. Inset: expansion of the responses from 0 to 10 RU. The amount of **ND** immobilized on the surface was 370 RU. (b) **NA**-immobilized sensor surface. The amount of **NA** immobilized on the surface was 1900 RU.

**Table 1.** Melting temperature ($T_m$) of RNA in the absence of **ND**

| RNA sequence | $T_m$ (°C) | | $\Delta T_m$ (°C) |
|---|---|---|---|
| | RNA | RNA + **ND** | |
| 5′-r(CUAACGGAAUG)-3′<br>3′-r(GAUUGCCUUAC)-5′ | 48.7 | 47.9 | −0.8 |
| 5′-r(CUAACGGAAUG)-3′<br>3′-r(GAUUGGCUUAC)-5′ | 33.5 | 38.3 | 4.8 |
| 5′-r(CUAACG GAAUG)-3′<br>3′-r(GAUUGC CUUAC)-5′<br>**U** | 36.0 | 36.5 | 0.5 |
| 5′-r(CUAACG GAAUG)-3′<br>3′-r(GAUUGC CUUAC)-5′<br>**A** | 35.1 | 35.2 | 0.1 |
| 5′-r(CUAACG GAAUG)-3′<br>3′-r(GAUUGG CUUAC)-5′<br>**U** | 30.6 | 39.7 | 9.1 |
| 5′-r(CUAAC GGAAUG)-3′<br>3′-r(GAUUG GCUUAC)-5′<br>**U** | 29.3 | 38.1 | 8.8 |
| 5′-r(CUAACG GAAUG)-3′<br>3′-r(GAUUGG CUUAC)-5′<br>**A** | 26.4 | 35.0 | 8.6 |
| 5′-r(CUAAC GGAAUG)-3′<br>3′-r(GAUUG GCUUAC)-5′<br>**A** | 26.8 | 35.4 | 8.6 |

The UV–melting curves were measured for duplexes (4 μM) in 10 mM sodium cacodylate buffer (pH 7.0) containing 100 mM NaCl in the absence and presence of ND (100 μM). Temperature was increased at a rate of 1 °C/min.

The N-terminal was fluorescently labeled with 5,6-TAMRA, whereas C-terminal was amidated. Upon addition of **hpRRE**, fluorescence anisotropy of **tamRev** (100 nM) increased markedly with increasing concentrations of **hpRRE** up to 160 nM, above which anisotropy exhibited a plateau, indicating formation of a complex (**tamRev–hpRRE**) (Fig. 3a). Using a nonlinear regression analysis of the binding curve reported earlier,[6,18] the dissociation constant of the **tamRev–hpRRE** complex was determined to be 5.6 nM. To examine inhibitory activities of the ligands on the formation of the **tamRev–hpRRE** complex, we measured the decrease in fluorescence anisotropy of a pre-formed **tamRev–hpRRE** complex upon titrating with the ligands. A release of bound **tamRev** from the complex by ligand displacement resulted in a decrease of fluorescence anisotropy. Upon titrating the **tamRev–hpRRE** complex with **ND**, **NA**, and neomycin B, a decrease in fluorescence anisotropy was

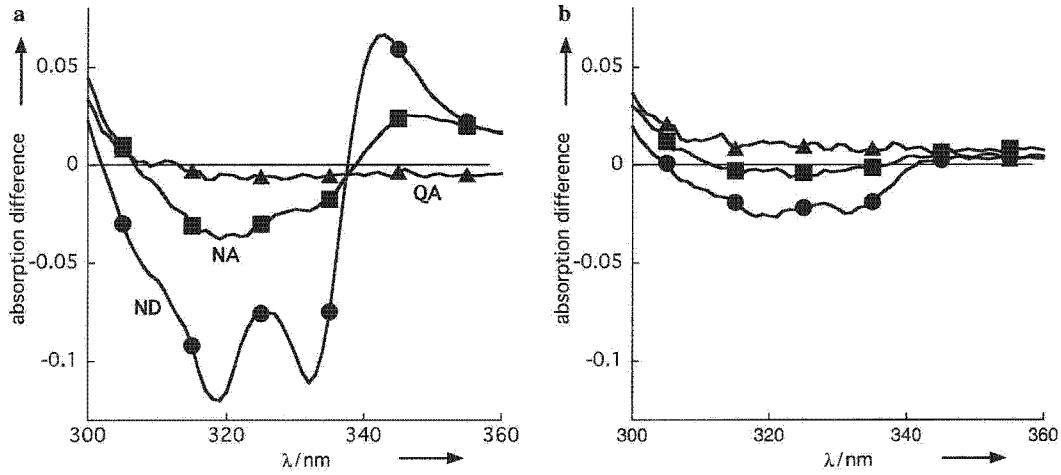


**Figure 2.** Difference UV spectra of ligands (20 μM) in the presence of (a) **hpRRE** (2 μM) and (b) **nRRE** (2 μM) in sodium phosphate (pH 7.0) containing EDTA (1 mM) and NaCl (100 mM). Key: **ND** (circle); **NA** (square); **QA** (triangle).

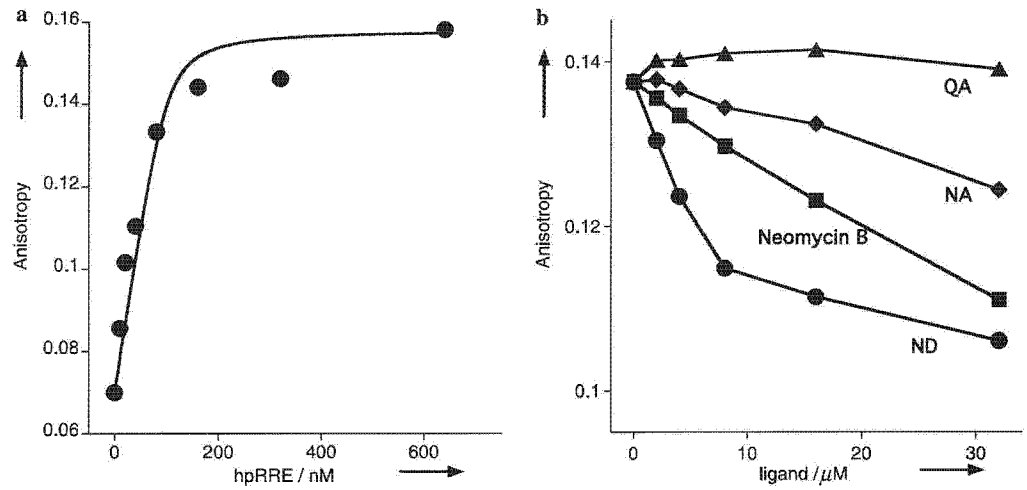


**Figure 3.** Fluorescence anisotropy assay. (a) A change of fluorescence anisotropy of **tamRev** (100 nM) (circle) titrated with **hpRRE**. Concentrations of **hpRRE** were 0, 10, 20, 40, 80, 160, 320, and 640 nM. The solid line represents a calculated binding curve obtained by a nonlinear regression analysis of the raw data. (b) Decreases of anisotropy by titrating the pre-formed complex between **hpRRE** (100 nM) and **tamRev** (100 nM) with ligands. Ligand concentrations were 0, 2, 4, 8, 16, and 32 μM. Key: **ND** (circle), **NA** (diamond), neomycin B (square), and **QA** (triangle).

observed, but not with **QA** (Fig. 3b). The dissociation of the **tamRev–hpRRE** complex was induced by **ND** much more efficiently than by neomycin B and **NA**.

## 3. Conclusion

The data reported here showed that (1) ligands binding to G-G and G-A mismatches in duplex DNA could also bind to a stem-loop IIB of RRE and (2) **ND** showed a stronger inhibitory activity for **tamRev–hpRRE** formation than neomycin B. While the precise mode of the binding as well as the binding stoichiometry of **ND** could not be determined by SPR and mass spectrometry, **ND** and **NA** were found useful to capture HIV-1 RRE when these molecules were immobilized on the surface. In addition, these results suggested that structural optimization of **ND** and **NA** toward the binding to the internal loop may lead molecules showing potent inhibitory activities against Rev–RRE binding.

## 4. Experimental

### 4.1. Substrates

All RNAs were purchased from PROLIGO with HPLC purification. 5,6-TAMRA-labeled peptide model was custom synthesized by Biosource International Inc. (Camarillo, California) with a purity of >95%.

### 4.2. General procedure for SPR-binding experiments

All measurements were carried out at 25 °C in a continuous flow of HBS-N buffer (10 mM HEPES, pH 7.4) containing NaCl (150 mM) at a flow rate of

30 μL/min. RNA samples (0.1 μM) in HBS-N buffer were heat denatured, folded by slow cooling, and injected into the sensor for 3 min to analyze the association to the surface. Then, the dissociation of the bound RNA to the surface was analyzed by injecting buffer only.

### 4.3. UV measurements

All UV measurements were carried out with SHIMADZU UV-2550 (Kyoto, Japan) at 25 °C.

**4.3.1. Sample preparation. hpRRE, hpTar, ssRNA,** and **nRRE** (2 μM) were denatured at 90 °C and cooled down slowly to a room temperature in a buffer (3.75 mM Na-phosphate, pH 7.0, 100 mM NaCl, 1.0 mM EDTA). A solution of ligand (20 μM) was added to the solution and left for 1 h at 25 °C. UV spectra were measured for each ligand with or without RNA. The difference UV spectra were obtained by subtracting the data in the presence of RNA from the data in the absence of RNA.

### 4.4. Fluorescence anisotropy assay

Fluorescence Anisotropy assays were carried out with a Beacon2000 system (Invitrogen) at 25 °C.

**4.4.1. tamRev–hpRRE binding. hpRRE** was denatured at 90 °C and cooled down slowly to a room temperature in a buffer (30 mM HEPES, pH 7.5, 10 mM Na-phosphate, pH 7.5, 100 mM KCl, 10 mM $NH_4OAc$, 0.1% Nonidet NP-40, 10 mM guanidine·HCl, 2 mM $MgCl_2$, 20 mM NaCl, 0.5 mM EDTA). To the solution of variable concentrations of **hpRRE** (10, 20, 40, 80, 160, 320, and 640 nM), **tamRev** (100 nM) was added and left for 12 h at 25 °C. Fluorescence anisotropy of the complex was measured with Beacon2000 at 25 °C. Average read cycles for the measurements were set to 10. The range control was auto.

**4.4.2. Inhibition assay. tamRev–hpRRE** complex was prepared by mixing 100 nM of each **tamRev** and **hpRRE** in a buffer as described above. A varing concentration of ligand (2, 4, 8, 16, and 32 μM) was added to the solution of **tamRev–hpRRE**, and the whole solution was left at 25 °C for 12 h. Fluorescence anisotropy was measured as above.

**4.4.3. Curve fitting.** Non-linear regression analysis for the **tamRev–hpRRE** formation was carried out by SigmaPlot2001 by using the equation for the 1:1 binding as shown below:

$$A_{obs} = (A_{max} - A_0) \cdot \alpha + A_0,$$

$$\alpha = \frac{([Rev]_0 + [RRE]_0 + K_d) \pm \sqrt{([Rev]_0 + [RRE]_0 + K_d)^2 - 4 \cdot [Rev]_0 \cdot [RRE]_0}}{2 \cdot [Rev]_0},$$

where $A_0$ and $A_{max}$ are anisotropy observed at 0 and 600 nM of **hpRRE**. $[Rev]_0$ and $[RRE]_0$ are the total concentration of each. $K_d$ is the dissociation constant, whereas $\alpha$ is the molar fraction of Rev–RRE complex against $[Rev]_0$.


## Acknowledgment

Authors thank Dr. Fumie Takei for the experimental assistance.


## References and notes


1. Pollard, V. M.; Malim, M. H. *Annu. Rev. Microbiol.* **1998**, *52*, 491–532.
2. Malim, M. H.; Böhnlein, S.; Hauber, J.; Cullen, B. R. *Cell* **1989**, *58*, 205–214.
3. Daly, T. J.; Cook, K. S.; Gray, G. S.; Maione, T. E.; Rusche, J. R. *Nature* **1989**, *342*, 816–819.
4. Bartel, D. P.; Zapp, M. L.; Green, M. R.; Szostak, J. W. *Cell* **1991**, *67*, 529–536.
5. Iwai, S.; Pritchard, C.; Mann, D. A.; Karn, J.; Gait, M. J. *Nucleic Acids Res.* **1992**, *20*, 6465–6472.
6. Luedtke, N. W.; Tor, Y. *Angew. Chem., Int. Ed.* **2000**, *39*, 1788–1790.
7. Kirk, S. R.; Luedtke, N. W.; Tor, Y. *J. Am. Chem. Soc.* **2000**, *122*, 980–981.
8. Hendrix, M.; Priestley, E. S.; Joyce, G. F.; Wong, C.-H. *J. Am. Chem. Soc.* **1997**, *119*, 3641–3648.
9. Zaman, G. J. L.; Michiels, P. J. A.; van Boeckel, C. A. A. *Drug Discovery Today* **2003**, *8*, 297–306.
10. Gallego, J.; Varani, G. *Acc. Chem. Res.* **2001**, *34*, 836–843.
11. Tok, J. B. H.; Bi, L. R.; Saenz, M. *Bioorg. Med. Chem. Lett.* **2005**, *15*, 827–831.
12. Nakatani, K.; Sando, S.; Saito, I. *Nat. Biotechnol.* **2001**, *19*, 51–55.
13. Nakatani, K.; Sando, S.; Kumasawa, H.; Kikuchi, J.; Saito, I. *J. Am. Chem. Soc.* **2001**, *123*, 12650–12657.
14. Hagihara, S.; Kumasawa, H.; Goto, Y.; Hayashi, G.; Kobori, A.; Saito, I.; Nakatani, K. *Nucleic Acids Res.* **2004**, *32*, 278–286.
15. Nakatani, K.; Hagihara, S.; Goto, Y.; Kobori, A.; Hagihara, M.; Hayashi, G.; Kyo, M.; Nomura, M.; Mishima, M.; Kojima, C. *Nat. Chem. Biol.* **2005**, *1*, 39–43.
16. Luedtke, N. W.; Tor, Y. *Biopolymers* **2003**, *70*, 103–119.
17. Lacourciere, K. A.; Stivers, J. T.; Marino, J. P. *Biochemistry* **2000**, *39*, 5630–5641, With a short RRE construct, neomycin showed $K_i$ value of 2 μM for inhibition of Rev binding. The highest affinity site of RRE for neomycin-binding ($K_d$ = 0.24 μM) was not disruptive to Rev-binding.
18. Sevenich, F. W.; Langowski, J.; Weiss, V.; Rippe, K. *Nucleic Acids Res.* **1998**, *26*, 1373–1381.

DNA Hybridization

DOI: 10.1002/anie.200601190

# Mismatch-Binding Ligands Function as a Molecular Glue for DNA**

*Tao Peng, Chikara Dohno, and Kazuhiko Nakatani**

Single-stranded DNA (ssDNA) hybridizes with another ssDNA unit having the complementary base sequence. The high sequence specificity in the hybridization is one of the most important properties of DNA as a genetic material, and also characterizes DNA as the unique component of the molecular architecture.[1–5] The formation of a double-stranded DNA (dsDNA) molecule of fully matched base sequences is highly energetically favorable and proceeds spontaneously at a temperature below the melting temperature ($T_m$) of the duplex, and therefore it is difficult to turn the hybridization on and off under isothermal conditions. Studies toward controlling or modulating the DNA hybridization with photochemical[6–9] and electronic reactions[10,11] of chemically modified oligonucleotides have been reported. Herein, we describe an approach to turn on duplex formation of two natural, unmodified ssDNA sequences that do not spontaneously hybridize with each other by a mismatch-binding ligand (MBL).

Recent studies on the binding of an MBL to the $(CGG)_n$ trinucleotide repeat revealed a novel mode of ligand binding to a mismatched DNA duplex.[12,13] The naphthyridine carbamate dimer (**NC**) selectively binds to the 5′-CGG-3′/5′-CGG-3′ sequence (CGG/CGG), which involves a G–G mismatch flanked by two C–G base pairs, with a 2:1 **NC**/DNA stoichiometry. The binding of **NC** to the CGG/CGG sequence induced two cytosines to be out of the π stack, as evidenced by the selective cleavage at the unpaired cytosine triggered by the addition of hydroxylamine.[12] We anticipated that the flipped-out cytosine in the **NC**-bound CGG/CGG triad could be substituted with other nucleotide bases such as thymine, and therefore **NC** could stabilize the 5′-TGG-3′/5′-TGG-3′ (TGG/TGG) sequence that consists of three contiguous T–G, G–G, and G–T mismatches (Figure 1). As the hybridization of two ssDNA molecules to produce the TGG/TGG sequence would be energetically unfavorable, these ssDNA sequences could be adhered by binding of **NC** to the TGG/TGG sequence.

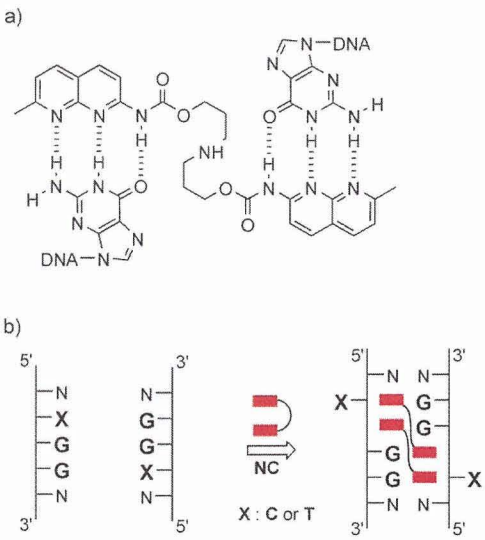


***Figure 1.*** a) **NC** and its hydrogen-bonding pattern to a guanine–guanine mismatch. b) Schematic representation of the binding of **NC** to the XGG/XGG sequence. Red rectangles: naphthyridine rings.

The binding of **NC** was first investigated for 5′-TGG-3′/5′-CGG-3′ (TGG/CGG) where one cytosine of the CGG/CGG sequence was substituted with thymine. The 11-mers 5′-d(CCCATGGTCCG)-3′ (**T1**) and 5′-d(CGGACGGTGGG)-3′ (**C1**; 5 μM) produced a duplex (**T1/C1**) containing a TGG/CGG sequence with a $T_m$ of 35.7 °C in sodium cacodylate buffer. In the presence of **NC**, the $T_m$ of the **NC**-bound **T1/C1** was 71.1 °C, which shows an increase in $T_m$ of 35.4 K (Figure 2). The transition from dsDNA to ssDNA is monophasic, regardless of the presence of **NC**. The transition occurred somewhat less cooperatively in the presence of **NC**. The melting kinetics may not be as simple as those in the

[*] Dr. T. Peng, Dr. C. Dohno, Prof. K. Nakatani
Department of Regulatory Bioorganic Chemistry
The Institute of Scientific and Industrial Research (SANKEN)
Osaka University
8-1 Mihogaoka, Ibaraki 567-0047 (Japan)
Fax: (+81) 6-6879-8459
E-mail: nakatani@sanken.osaka-u.ac.jp

[**] This work was supported by a Grant-in-Aid for Scientific Research (A) from the Japan Society for the Promotion of Science, Health and Labor Sciences Research Grants for Research on Advanced Medical Technology from the Ministry of Health, Labor, and Welfare, and CREST, Japan Science and Technology Agency.

Supporting information for this article is available on the WWW under http://www.angewandte.org or from the author.

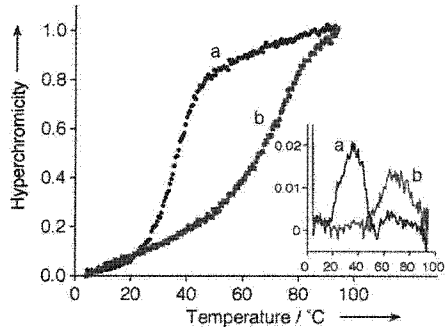


*Figure 2.* Thermal denaturation profile of **T1** and **C1** (5 μM each) in the absence (a) and presence (b) of **NC** (100 μM). The absorbance at 260 nm was measured in sodium cacodylate buffer (10 mM, pH 7.0) containing 0.1 M NaCl. The temperature was increased from 4 to 94 °C at a rate of 1 °C min$^{-1}$. The absorbance was measured with an interval of 1 °C. Measurements were carried out at least three times. The average of three data sets of denaturation profiles was used for the plots. Inset: differential plots of the melting profiles.

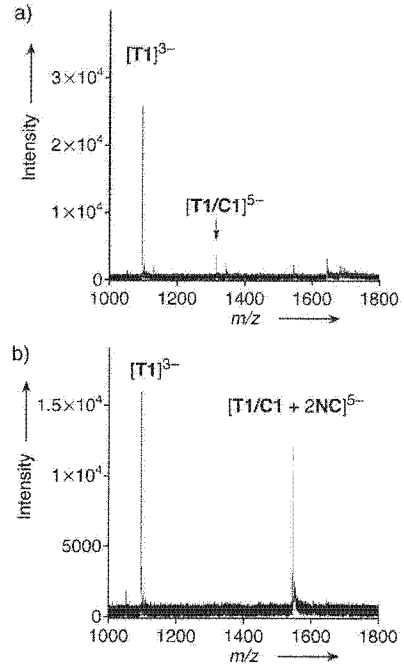


*Figure 3.* CSI-TOF MS of **T1** and **C1** in the a) absence and b) presence of **NC** (40 μM). Samples contained 20 μM of each strand in 50% aqueous methanol and ammonium acetate (100 mM). Ions in the range of *m/z* from 1000 to 1800 are shown for clarity. The sample solution was cooled at −10 °C during the injection with a flow rate of 0.5 mL h$^{-1}$.

absence of **NC**, because this transition involves the dissociation of four components, two DNA strands (**T1** and **C1**) and two **NC** molecules. The thermal denaturation profiles showed that in the temperature range between 45 and 55 °C, **T1** and **C1** were present as single-stranded forms in the absence of **NC** but as an **NC**-bound duplex form in the presence of **NC**.

The cold-spray ionization time-of-flight mass spectrometry (CSI-TOF MS)[12,14] of **T1** and **C1** showed ions corresponding to a 3− ion of a single-stranded form ($[\mathbf{T1}]^{3-}$, *m/z*: found: 1096.2; calcd: 1096.2) and a 5− ion of a duplex form ($[\mathbf{T1/C1}]^{5-}$, *m/z*: found: 1344.8; calcd: 1344.6; Figure 3a). On addition of **NC** to the duplex with a 2:1 molar ratio, the intensity of the ions corresponding to $[\mathbf{T1}]^{3-}$ became weaker with the concomitant appearance of a new ion corresponding to the 5− ion of a 2:1 complex of **NC** and the duplex ($[\mathbf{T1/C1}+2\mathbf{NC}]^{5-}$, *m/z*: found: 1546.3; calcd: 1545.9; Figure 3b). On increasing the concentration of **NC**, the intensity of the ion corresponding to $[\mathbf{T1/C1}+2\mathbf{NC}]^{5-}$ became strong with a concomitant decrease of the intensity of $[\mathbf{T1}]^{3-}$ (see Supporting Information). Complexes of **NC** bound to **T1/C1** with 1:1 and/or 3:1 stoichiometries were not detected. These results clearly showed that the binding of **NC** to the duplex **T1/C1** proceeded in an exclusive stoichiometry of 2:1. This stoichiometry of **NC** binding is the characteristic feature that is observed for the binding of **NC** to the CGG/CGG sequence[12] and the binding of the related MBL naphthyridine azaquinolone to the CAG/CAG sequence. The structure of the latter complex has been determined by NMR spectroscopy.[13] These findings suggested that the thymine in the **NC**-bound **T1/C1** would most likely be out of the π stack.

The T component in the extrahelical position could be preferentially oxidized with potassium permanganate ($KMnO_4$) compared to that in the intrahelical position.[15] The resulting thymine glycol (Tg) can be degraded with hot piperidine, eventually leading to strand cleavage.[16–18] The oxidation of **T1/C1** with $KMnO_4$ followed by treatment with hot piperidine was examined (Scheme 1). The duplex **T1/C1** (12.5 μM) did not react with $KMnO_4$ (0.2 mM) at 0 °C for

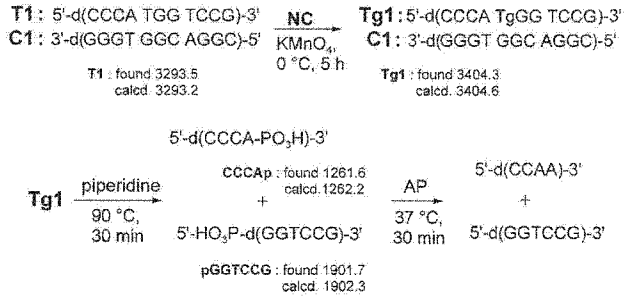


*Scheme 1.* The oxidation of **T1/C1** by $KMnO_4$ upon binding of **NC**. AP = alkaline phosphatase.

320 min, as judged by reversed-phase HPLC analysis (see Supporting Information). In contrast, the TGG-containing DNA **T1** was consumed by 70% in the presence of **NC** (40 μM) and converted into the 11-mer DNA 5′-d(CCCA-TgGGTCCG)-3′ (**Tg1**) which contained a Tg unit.[16] After isolation by HPLC, **Tg1** was treated with hot piperidine to give two products corresponding to oligomers 5′-d(CCCA)-$PO_3H$-3′ (**CCCAp**) and 5′-$HO_3P$-d(GGTCCG)-3′ (**pGGTCCG**). All DNA products were identified by MALDI-TOF mass spectrometry (Scheme 1). Although the duplex **T1/C1** contained two kinds of thymine residues, only that in the TGG/CGG sequence was reactive to $KMnO_4$ upon **NC** binding. These results clarified the finding that the T unit in the TGG/CGG sequence was in the extrahelical position in the **NC**-bound complex.

  

Having confirmed that 1) **NC** could stabilize the duplex containing two contiguous T–G and G–G mismatches in **T1/C1** and 2) the T component was in the extrahelical position in the **NC**-bound TGG/CGG sequence, the binding of **NC** to the three contiguous mismatches T–G, G–G, and G–T in the TGG/TGG sequence was investigated. The 11-mers 5′-d(CCTTTGGTCAG)-3′ (**T2**) and 5′-d(CTGATGGAAGG)-3′ (**T3**) that had a 5′-TGG-3′ sequence were present as single-stranded forms at room temperature, as shown by the denaturation profile, because the possible duplex **T2/T3** should involve three contiguous mismatches (Figure 4a). At

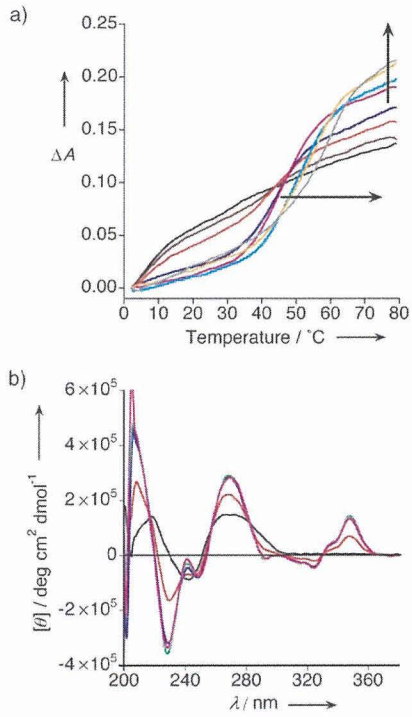


***Figure 4.*** a) Thermal denaturation profile of **T2** and **T3** (5 μM each) with different concentrations of **NC** (0 (black), 2.5 (brown), 5 (red), 10 (blue), 20 (purple), 40 (cyan), 60 (yellow), and 100 μM (gray)). The vertical arrow indicates the increase in $\Delta A$ with increasing **NC** concentration. The horizontal arrow indicates the increase in melting temperature with increasing **NC** concentration. b) CD spectrum of **T2** and **T3** (5 μM each) measured in sodium cacodylate buffer (10 mM, pH 7.0) and NaCl (100 mM) at 25 °C in the absence (black) and presence of **NC** at 5 μM (red), 10 μM (blue), 15 μM (green), and 20 μM (purple).

increasing concentrations of **NC**, the transition from dsDNA to ssDNA became apparent and shifted toward a higher-temperature region. Notably, the $T_m$ value for **T2** and **T3** reached 58.8 °C in the presence of 100 μM **NC**, thus showing the formation of a stable, **NC**-bound **T2/T3** duplex at room temperature.

The transition of ssDNA to dsDNA of **T2** and **T3** during titration with **NC** was monitored by circular dichroism (CD) spectroscopy (Figure 4b). Without **NC**, the CD spectrum of the mixture of **T2** and **T3** showed a positive band at 272 nm and a negative band at 250 nm. After addition of **NC**, the ellipticity of the positive band increased on increasing the amount of **NC** from one to four molar equivalents. In addition, the induced CD bands observed at 348 and 324 nm also changed their magnitude in response to the **NC** concentration. The change in CD involved the isodichroic points, and showed the transition of single-stranded **T2** and **T3** to the **NC**-bound duplex. The formation of the **NC**-bound duplex was further supported by CSI-TOF MS observations which indicated a 2:1 complex of **NC** with **T2/T3**. Again, the stoichiometry was exclusively 2:1. A selective strand cleavage of the 11-mer 5′-d(GCAATGGTTGC)-3′ (**T4**) at the T component in the TGG/TGG sequence was also confirmed by $KMnO_4$ oxidation upon binding of **NC** to the **T4/T4** duplex followed by heating with piperidine. In contrast, the protection of the other two T units from oxidation by $KMnO_4$ indicated that these components are in the intrahelical position (see Supporting Information).

The results described herein showed that **NC** could stabilize not only the two contiguous T–G and G–G mismatches in the TGG/CGG sequence, but also the three contiguous T–G, G–G, and G–T mismatches in the TGG/TGG sequence. By choosing an appropriate DNA sequence, two ssDNA molecules that do not spontaneously hybridize with each other could be adhered by the binding of **NC** to the TGG/TGG sequence. On the basis of **NC** binding to the CGG/CGG sequence, we used the TGG/TGG sequence in which the C component is substituted with another pyrimidine nucleotide base. In fact, the C component in the CGG/CGG sequence could be substituted with purine bases A and G, as evidenced by the CSI-TOF MS of the **NC**-bound complex for the AGG/AGG and GGG/GGG sequences. These results will be reported elsewhere. The molecule **NC** represents a new class of substances that function as molecular glue, not only in DNA hybridization but also in modulating the DNA secondary structure.

Received: March 25, 2006
Revised: May 26, 2006
Published online: July 21, 2006

**Keywords:** DNA · hybridization · mass spectrometry · nucleotides

[1] E. Winfree, F. Liu, L. A. Wenzler, N. C. Seeman, *Nature* **1998**, *394*, 539–544.
[2] B. Yurke, A. J. Turberfield, A. P. Mills, Jr., F. C. Simmel, J. E. Neumann, *Nature* **2000**, *406*, 605–608.
[3] H. Yan, S. H. Park, G. Finkelstein, J. H. Reif, T. H. LaBean, *Science* **2003**, *301*, 1882–1884.
[4] M. Endo, T. Majima, *Angew. Chem.* **2003**, *115*, 5922–5925; *Angew. Chem. Int. Ed.* **2003**, *42*, 5744–5747.
[5] S. Liao, N. C. Seeman, *Science* **2004**, *306*, 2072–2074.
[6] B. Ghosn, F. R. Haselton, K. R. Gee, W. T. Monroe, *Photochem. Photobiol.* **2005**, *81*, 953–959.
[7] H. Asanuma, T. Ito, T. Yoshida, X. Liang, M. Komiyama, *Angew. Chem.* **1999**, *111*, 2547–2549; *Angew. Chem. Int. Ed.* **1999**, *38*, 2393–2395.
[8] H. Asanuma, X. Liang, T. Yoshida, A. Yamazawa, M. Komiyama, *Angew. Chem.* **2000**, *112*, 1372–1374; *Angew. Chem. Int. Ed.* **2000**, *39*, 1316–1318.
[9] X. G. Liang, H. Asanuma, M. Komiyama, *J. Am. Chem. Soc.* **2002**, *124*, 1877–1883.

  

[10] K. Hamad-Schifferli, J. J. Schwartz, A. T. Santos, S. G. Zhang, J. M. Jacobson, *Nature* **2002**, *415*, 152–155.
[11] J. Yang, J. Y. Lee, H.-P. Too, G.-M. Chow, *Biophys. Chem.* **2006**, *120*, 87–95.
[12] T. Peng, K. Nakatani, *Angew. Chem.* **2005**, *117*, 7446–7449; *Angew. Chem. Int. Ed.* **2005**, *44*, 7280–7283.
[13] K. Nakatani, S. Hagihara, Y. Goto, A. Kobori, M. Hagihara, G. Hayashi, M. Kyo, M. Nomura, M. Mishima, C. Kojima, *Nat. Chem. Biol.* **2005**, *1*, 39–43.
[14] K. Yamaguchi, *J. Mass Spectrom.* **2003**, *38*, 473–490.
[15] H. Hayatsu, T. Ukita, *Biochem. Biophys. Res. Commun.* **1967**, *29*, 556–561.
[16] C. M. Rubin, C. W. Schmid, *Nucleic Acids Res.* **1980**, *8*, 4613–4620.
[17] A. M. Maxam, W. Gilbert, *Methods Enzymol.* **1980**, *65*, 499–560.
[18] J. A. Gogos, M. Karayiorgou, H. Aburatani, F. C. Kafatos, *Nucleic Acids Res.* **1990**, *18*, 6807–6814.

  

DOI: 10.1002/cbic.200600477

# Detection of L-DNA-Tagged PCR Products by Surface Plasmon Resonance Imaging

Gosuke Hayashi,[a, b] Masaki Hagihara,[a, b] Akio Kobori,[a, c] and Kazuhiko Nakatani*[a, b]

*Dedicated to Professor Isao Saito on the occasion of his 65th birthday.*

The employment of tags plays an increasingly important role in genomics, in which PCR products are arrayed at the micro- or nanoscale. PCR products have been labeled in many ways. One conventional method is to incorporate labeled nucleotides into the PCR products during the extension reaction by DNA polymerase. Another method is to use a PCR primer that is labeled at the 5′ end. PCR primers with fluorophore labels are used for DNA sequencing, whereas biotinylated primers are used for the isolation and detection of the PCR products due to their strong and specific binding to streptavidin. Here, we report on a mirror-image DNA (L-DNA)-tagged PCR (LT-PCR) that enables us to label the PCR products with a defined sequence of L-DNA tag. The important findings leading to LT-PCR were that the L-DNA tag did not interfere with the PCR and remained as a single strand even after PCR. Therefore, LT-PCR products could be precisely delivered onto the DNA microarray, where the L-DNA complementary to the tag sequence was immobilized. A large number of sequences available for L-DNA tags would be suitable for such comprehensive microarray analysis. We demonstrated that the surface plasmon resonance imaging (SPR) array carrying the complementary L-DNA on the surface successfully detected the LT-PCR products without any purification or additional fluorescent labeling.

L-DNA consisting of L-2′-deoxyriboses is an enantiomer of natural DNA (D-DNA) and has unique properties.[1] L-DNA has been shown to be a poor substrate for the human *endo*- and *exo*-nucleases, as it has the opposite chirality to their intrinsic target,[2] and does not interact with single-stranded D-DNA, whereas it does bind sequence-selectively to complementary L-DNA. We anticipated that an L-DNA tag attached to a PCR primer at the 5′-end would not be recognized as a PCR template by DNA polymerase and would remain in a single-stranded form after amplification (Scheme 1). Besides L-DNA, a peptide nucleic acid (PNA) or D-DNA tag attached through a nonreplicable linker were conceivable for coding PCR products. However, the binding ability of PNA or D-DNA to complementary D-DNA might induce the formation of undesirable intraprimer hairpins or an interaction to an unexpected sequence of the template DNA. The intrinsic possibility of forming hairpin secondary structures and ambiguity in the effect on the PCR reactions thus makes them unsuitable for the labeling.

Primers used in LT-PCR consist of three parts, D-DNA to function as a general PCR primer, a L-DNA unit as a molecular tag, and three L-dTs as a spacer between the D and L-DNA. The spacer was inserted to mitigate steric congestion that might be produced between the left-handed and the right-handed duplexes upon hybridization of LT-PCR products with a complementary L-DNA. LT primers were synthesized by a conventional protocol of chemical DNA synthesis with phosphoramidites of D- and L-2′-deoxyribonucleosides. L-deoxynucleosides were synthesized according to the reported procedures.[3] Synthesized LT primers were purified by HPLC and PAGE, and identified by MALDI-TOF MS and enzymatic digestion experiments (see Figure S1 in the Supporting Information). The primers and oligonucleotides used in our study are shown in Table 1.

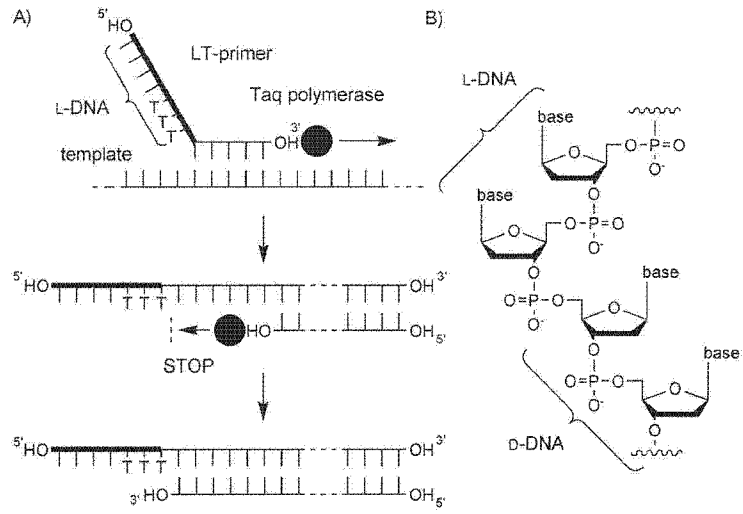


**Scheme 1.** An illustration of LT-PCR. A) The LT primer consists of an L-DNA sequence tag (thick line), a spacer of three L-dT nucleotides, and a D-DNA primer sequence (thin line). In the amplification reaction, DNA synthesis by Taq polymerase (●) stopped at the boundary between the L and D portions of the template. The products of LT-PCR contained a single-stranded L-DNA tag. B) Chemical structure at the boundary of D- and L-DNA in the LT primer.

LT-PCR with a primer set of L1-M13 and M13-RV was carried out with pUC18 plasmid as a template (Figure 1A). L1-M13 consisted of a 20-mer L-DNA tag, L-d(T)$_3$, and a 17-mer M13 forward primer sequence. The LT-PCR products obtained by L1-M13 and M13-RV showed slower migration on the nonde-

[a] G. Hayashi, Dr. M. Hagihara, Dr. A. Kobori, Prof. Dr. K. Nakatani
Department of Synthetic Chemistry and Biological Chemistry
Graduate School of Engineering, Kyoto University
Kyoto 615-8510 (Japan)

[b] G. Hayashi, Dr. M. Hagihara, Prof. Dr. K. Nakatani
Current address: Department of Regulatory Bioorganic Chemistry
The Institute of Scientific and Industrial Research, Osaka University
8–1 Mihogaoka, Ibaraki 567-0047 (Japan)
Fax: (+81) 6-6879-8459
E-mail: nakatani@sanken.osaka-u.ac.jp

[c] Dr. A. Kobori
Current address: Department of Biomolecular Engineering
Kyoto Institute of Technology (Japan)

Supporting information for this article is available on the WWW under http://www.chembiochem.org or from the author.

  

naturing PAGE analysis than 123 bp products obtained from a primer set of M13 and M13-RV (Figure 1B). The LT-PCR product showed two distinct bands in the denaturing PAGE analysis (Figure 1C). One band showed the same migration as that obtained by conventional PCR with a M13 primer set, whereas the other band showed slower migration. This result indicates that the LT-PCR products consisted of two DNA strands of different length. Since the migration of shorter DNA strand was almost the same as that of the PCR products produced from a M13 primer set, the DNA synthesis from the reverse primer M13-RV was most likely to stop around the boundary of D- and L-DNA on the template. The formation of two DNA strands of different length was also confirmed in LT-PCR carried out with a L2-GH and GH-RV primer set on pUC18 (Figure S2). The results were fully consistent with those obtained with a L1-M13 and M13-RV primer set.

Primer-extension experiments of 5′-FAM-labeled 13-mer (FAM13) further confirmed that Taq polymerase did not synthesize DNA on an L-DNA template (Figure S3). The product of the primer extension of FAM13 with an L1-M13 template was identified as FAM17 by denaturing PAGE analysis. MALDI-TOF MS also confirmed the formation of FAM17 but not any further elongated products, thus indicating that four nucleotides were added to the 3′-end of FAM13 on the template of D-DNA region but not a fifth. These results clarified that DNA synthesis by Taq polymerase on LT primer proceeded in the region of the D-DNA template but not in the region of the L-DNA template.

**Table 1.** Oligonucleotides used for our experiments.

| Name | Sequence (5′ to 3′)[a] |
|---|---|
| L1-M13 | $^{L}$(ATGCTACCGTATGCCCAGTGTTT)-$^{D}$(GTTTTCCCAGTCACGAC) |
| M13 | $^{D}$(GTTTTCCCAGTCACGAC) |
| M13-RV | $^{D}$(CAGGAAACAGCTATGAC) |
| B-M13-RV | biotin-$(CH_2)_6$-$^{D}$(CAGGAAACAGCTATGAC) |
| L1C | $^{L}$(CACTGGGCATACGGTAGCAT)-$(CH_2)_6$-SH |
| L2C | $^{L}$(TTGGCTCTGTCTCCGTTGTC)-$(CH_2)_6$-SH |

[a] Superscripts denote L- and D-DNA, respectively.

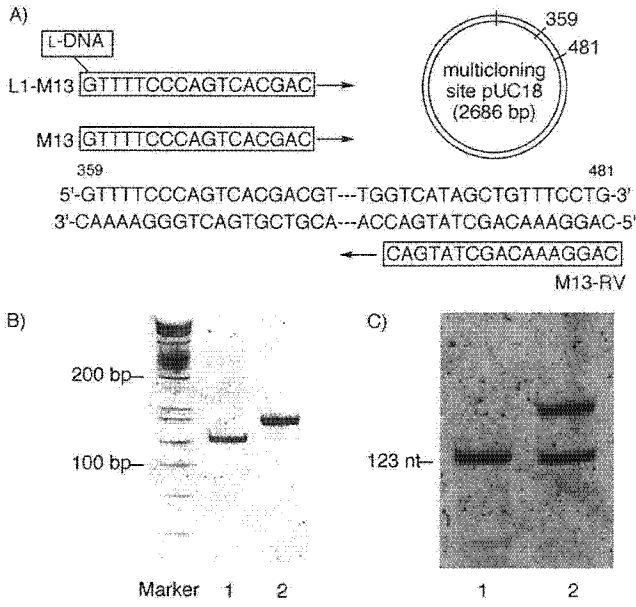


**Figure 1.** Analysis of LT-PCR products. A) Alignment of primers on pUC18. B) Native PAGE analysis of LT-PCR products obtained from a L1-M13 and M13-RV primer set (lane 2) and a 123 bp duplex obtained from a M13 and M13-RV primer set (lane 1). PCR products were loaded onto 10% polyacrylamide gel without any purification. Gel bands were stained by SYBR Green I. C) Denaturing PAGE analysis of the LT-PCR products. Lane 1, a PCR product from a M13 and M13-RV primer set; lane 2, a LT-PCR product obtained from a L1-M13 and M13-RV primer set. Gel bands were stained by SYBR Green II.

An identifiable L-DNA sequence tag that labeled the PCR products would be useful for isolating and detecting the desired PCR products in a duplex form. To demonstrate that the duplex form of the PCR products can be captured selectively at the designated position on the array surface, an SPR imaging array[4] carrying the complementary L-DNA to the L-DNA sequence tag was prepared. The 20-mer L-DNAs L1C and L2C, which were complementary to the L1 and L2 sequence tags, respectively, were synthesized with alkyl thiol modification at the 3′-end. L1C and L2C were immobilized onto the gold surface of sensor chips for the SPR imaging analysis (Figure 2A). After LT-PCR of pUC18 with two primer sets, each duplex of the LT-PCR products was separately applied onto the sensor surface without any purification procedures. When the LT-PCR products obtained from an L1-M13 and M13-RV primer set were applied to the SPR surface array, SPR signals were selectively detected on the L1C spots (Figure 2B), whereas distinct SPR signals were observed on the L2C spots when LT-PCR products obtained from a L2-GH and GH-RV primer set were applied (Figure 2C).

Under these experimental conditions, any L-DNA tagged primers that were not consumed in the PCR reaction should also bind to the complementary sequence on the array surface, because the PCR products were not purified prior to the array analyses. However, a sandwich assay with a secondary antibody clearly demonstrated that the observed SPR difference images were largely due to the binding of the duplex form of LT-PCR products on the SPR sensor surface. The assay exploited the 5′-biotinylated M13-RV (B-M13-RV) and L1-M13 for LT-PCR. The LT-PCR products were mixed with streptavidin (SA) and applied to the array surface. After complete hybridization of LT-PCR products, the successive addition of the antibody against SA to the surface resulted in a considerable increase in SPR intensity (Figure 2D). In contrast, virtually no signal increase was observed upon successive application of the mixture of L1-M13 and B-M13-RV without PCR and SA antibody (Figure 2E). These results proved that LT-PCR products could hybridize to complementary L-DNA immobilized on an array surface.

This report demonstrates that LT-PCR, a novel PCR technique, provides an efficient method for coding PCR products with a sequence-defined L-DNA tag. Without separation, purification, or denaturing–annealing processes, the products of LT-PCR could be captured in a duplex form on an SPR imaging surface array where L-DNA sequences complementary to tag sequences were immobilized. The LT-PCR and L-DNA SPR imaging array described here is just the first step in L-DNA tag technologies, which will be applicable to diverse molecular biology experiments.[5]

  

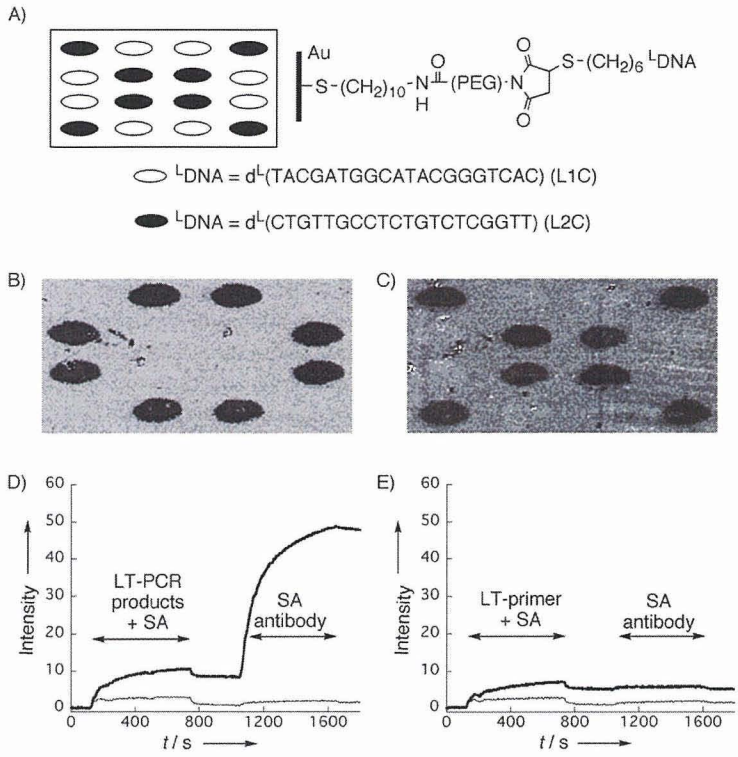


**Figure 2.** Detection of LT-PCR products on an L-DNA-immobilized SPR imaging array. A) Chemical structure of the L-DNA array surface and the immobilization pattern of L1C (○) and L2C (●). SPR difference images (between 30 and 600 s) obtained from LT-PCR products with B) a L1-M13 and M13-RV, and C) a L2-GH and GH-RV primer set. D) Sandwich assay with secondary antibody to SA. LT-PCR products obtained from a L1-M13 and B-M13-RV primer set were mixed with SA solution and applied to an L-DNA array. Significant interactions with the SA antibody were observed for the LT-PCR products. Key: signal at L1C, bold line; signal at the background spot, thin line. E) No interaction was observed for the solution without LT-PCR.

## Experimental Section

**LT-PCR:** L-DNA-tagged PCR on pUC18 plasmid was performed with a primer set of L1-M13 and M13-RV, or of L2-GH and GH-RV. The amplification reaction was carried out with 500 nM of each primer, 1×Taq PCR Master Mix Kit (Qiagen), and pUC18 (100 pg $\mu L^{-1}$). The amplification protocol was 94 °C for 3 min; 35 cycles of 94 °C for 30 s, 55 °C for 30 s, and 72 °C for 1 min; and then 72 °C for 7 min. The LT-PCR products were analyzed by native PAGE (10% polyacrylamide gel, stained by SYBR Green I) and denaturing PAGE (8% polyacrylamide gel containing 7 M urea, stained by SYBR Green II).

**Fabrication of the L-DNA-immobilized SPR imaging array:** A gold-coated chip (SPR-200) for SPR imaging analysis was purchased from Toyobo (Japan). 8-Aminooctane-1-thiol (200 μL, 1 mM, Dojindo, Japan) in ethanol was dripped onto the gold surface and allowed to react for more than 7 h. After being washed with ethanol and distilled water, the aminoalkyl-modified surface was treated for 2 h with the heterobifunctional cross-linker MAL-$PEG_{12}$-NHS ester (200 μL, 5 mg $mL^{-1}$, Quanta Biodesign) to create a maleimido-modified surface. Drops of thiol-terminated L-DNA (10 nL, 20 μM) were delivered automatically onto the maleimido surface by using an automated spotter (Toyobo). The maleimido–thiol coupling was allowed to proceed overnight. The array surface was further treated with PEG-thiol (200 μL, 400 μg) for 2 h to block any remaining maleimido groups, then rinsed with a phosphate buffer and water. A phosphate buffer (10 mM phosphate, pH 7.2, 150 mM NaCl) was used for all array fabrication reactions.

**SPR imaging analysis of LT-PCR products:** The L-DNA-immobilized SPR array was placed in the SPR imager (Toyobo, Japan). After the surface had been washed with NaOH for 2 min, running phosphate buffer was applied to the array for 100 s, then LT-PCR products in the running buffer were applied for 5 min with a flow speed of 100 μL $min^{-1}$. Running buffer was then applied for a further 5 min. All SPR experiments were performed at 30 °C. The SPR array was reused after being washed with NaOH (0.5 M) for 3 min. The SPR images and signal data were collected with a MultiSPRinter Analysis program (Toyobo). The SPR difference images were constructed by using Scion Image (Scion, MD, USA).

**Secondary antibody assay:** LT-PCR was carried out with a primer set of L1-M13 and B-M13-RV. The product (40 μL) was mixed with a solution of streptavidin in phosphate buffer (90 μL 2 M) and applied onto the L1C-immobilized SPR surface array for 10 min. The array surface was further exposed to the SA antibody (20 μg $mL^{-1}$) for 10 min. For the negative control, the LT-PCR solution was analyzed by the same procedure without running the PCR amplification.

## Acknowledgements

*We are grateful to Toyobo Bio-laboratory for their instructions for SPR imaging experiments.*

**Keywords:** chirality · DNA · polymerase chain reaction · surface plasmon resonance

[1] a) S. Fujimori, K. Shudo, Y. Hashimoto, *J. Am. Chem. Soc.* **1990**, *112*, 7436–7438; b) H. Urata, K. Shinohara, E. Ogura, Y. Ueda, M. Akagi, *J. Am. Chem. Soc.* **1991**, *113*, 8174–8175; c) M. Doi, M. Inoue, K. Tomoo, T. Ishida, Y. Ueda, M. Akagi, H. Urata, *J. Am. Chem. Soc.* **1993**, *115*, 10423–10433; d) A. Garbesi, B. L. Capobianco, F. P. Colonna, L. Tondelli, F. Arcamone, G. Manzini, C. W. Hilbers, J. M. E. Aelen, M. J. J. Blommers, *Nucleic Acids Res.* **1993**, *21*, 4159–4165; e) W. G. Purschke, F. Radtke, F. Keinjung, S. Klussmann, *Nucleic Acids Res.* **2003**, *31*, 3027–3032.

[2] K. P. Williams, X. Liu, T. N. M. Schumacher, H. Y. Lin, D. A. Ausiello, P. S. Kim, D. P. Bartel, *Proc. Natl. Acad. Sci. USA* **1997**, *94*, 11285–11290.

[3] a) H. Urata, E. Ogura, K. Shinohara, Y. Ueda, M. Akagi, *Nucleic Acids Res.* **1992**, *20*, 3325–3332; b) G. S. Ti, B. L. Gaffney, R. A. Jones, *J. Am. Chem. Soc.* **1982**, *104*, 1316–1319; c) Z. Shi, B. Yang, Y. Wu, *Tetrahedron* **2002**, *58*, 3287–3296.

[4] a) A. J. Thiel, A. G. Frutos, C. E. Jordan, R. M. Corn, L. M. Smith, *Anal. Chem.* **1997**, *69*, 4948–4956; b) K. Motoki, T. Yamamoto, H. Motohashi, T. Kamiya, T. Kuroita, T. Tanaka, J. D. Engel, B. Kawakami, M. Yamamoto, *Genes Cells* **2004**, *9*, 153–164; c) T. T. Goodrich, H. J. Lee, R. M. Corn, *J. Am. Chem. Soc.* **2004**, *126*, 4086–4087.

[5] Note added in proof. Independent work on the PCR with an L-DNA tag was recently reported. N. C. Hauser, R. Martinez, A. Jacob, S. Rupp, J. D. Hoheisel, S. Matysiak, *Nucleic Acids Res.* **2006**, *34*, 5101–5111.

Received: November 9, 2006
Published online on December 29, 2006

  

DOI: 10.1002/cbic.200700005

# Bidirectional Control of Gold Nanoparticle Assembly by Turning On and Off DNA Hybridization with Thermally Degradable Molecular Glue

Tao Peng, Chikara Dohno, and Kazuhiko Nakatani*[a]

Hybridization of single-stranded DNA (ssDNA) with its complementary strand is important not only in many biological processes but also in DNA-based bioassays and nanodevices.[1–5] The high sequence specificity of hybridization has also been applied to the construction of nanometer-scale structures[6–8] and DNA-based molecular machines that include controlled motion of DNA.[9–11] Modulation and control of the formation of double-stranded DNA (dsDNA) is a general strategy for enhancing, limiting, or triggering these biological processes and functions. Several methods have been reported for the control of DNA hybridization by using photochemical[12–14] and electronic[15,16] reactions on chemically modified DNA. We have introduced the concept of "molecular glue" for the mediation of hybridization of unmodified DNA with synthetic small molecules that bind to sequences containing up to three contiguous base mismatches. Molecular glue can adhere to two unmodified ssDNA molecules that do not hybridize with each other.[17,18] The function of the molecular glue that we previously reported relied on thermodynamically favorable ligand binding to two ssDNA molecules.[17] Its function did not include the denaturation of the duplex once formed, and was limited to the unidirectional control of DNA hybridization. To achieve bidirectional control, that is, to turn DNA hybridization on and off, we have looked for methods to inactivate the molecular glue in the reaction system. Here, we describe bidirectional control of DNA hybridization by using the new thermally degradable molecular glue, TD (Scheme 1). Irreversible thermal conversion of TD into its inactive form allowed us to control the DNA hybridization/denaturation cycle. This method for turning DNA hybridization on and off was then applied to the control of the assembly of gold nanoparticles.

TD consists of two naphthyridine heterocycles that recognize guanine and selectively bind to dsDNA molecules with G–G mismatches. A key feature of TD, compared to the molecular glue previously reported, is its ability to function as a glue for DNA at room temperature but then be inactivated at an elevated temperature. In order to acquire inactivation, we modified the structure of the original molecule and found that, at an elevated temperature, the bond that connects the two naphthyridine heterocycles can be removed, which remarkably results in the inactivation of the glue function.[19] Thermolysis of TD in 10 mM sodium cacodylate buffer (pH 7.0), as monitored by reversed-phase HPLC, showed that TD was completely consumed within 4 min incubation at 80 °C with concomitant formation of two products (Figure 1). The products were identified as 2-amino-7-methyl-1,8-naphthyridine (**1**) and (7-methyl-1,8-naphthyridin-2-yl)-carbamic acid 2-(2-oxo-oxazolidin-3-yl)-ethyl ester (**2**; Figure 1B). The formation of **1** and **2** indicated that TD underwent thermal fragmentation by an intramolecular carbamate exchange. These results showed that TD could be irreversibly transformed to **1** and **2** by simple heating, and was therefore no longer effective in stabilizing dsDNA.

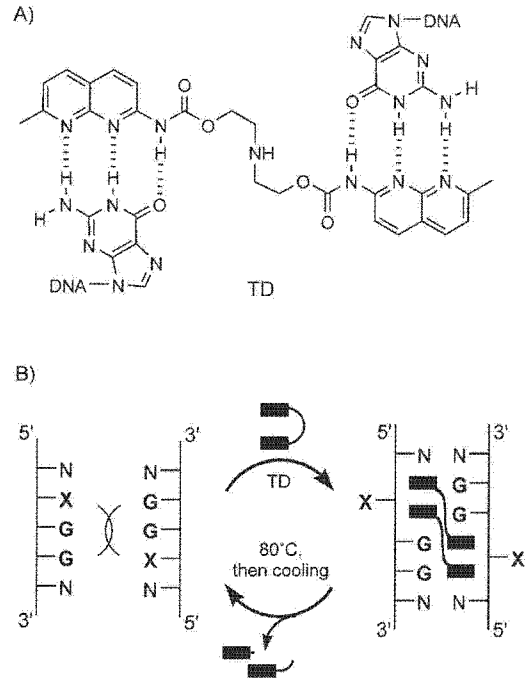


**Scheme 1.** A) The structure of TD and its hydrogen-bonding pattern with guanines on opposing strands of a DNA duplex. B) Schematic representation of TD-assisted hybridization of two ssDNA molecules that contain the sequences 5′-XGG and 5′-XGG (X = C or T), and denaturation of TD-bound dsDNA by heat-induced inactivation of TD followed by gradual cooling to room temperature. The X bases in the XGG/XGG sequence are expected to be flipped-out of the helix, as shown on the right-hand side of the arrow.

The function of TD as a molecular glue for DNA was confirmed by measuring the melting temperature ($T_m$) of 11-mer duplexes (5′-d(CTA ACX GAA TG)-3′/5′-d(CAT TCY GTT AG)-3′) that contained mismatches. Experiments were carried out with all possible combinations of matched and mismatched base pairs (represented by X–Y in the sequences) in the absence and presence of TD. TD selectively bound to the dsDNA that contained the G–G mismatch (X = Y = G; see the Supporting Information). In the presence of 100 μM TD, the $T_m$ increase ($\Delta T_m$) for the duplex that contained the G–G mismatch was 25.7 °C;

[a] *Dr. T. Peng, Dr. C. Dohno, Prof. K. Nakatani*
*Department of Regulatory Bioorganic Chemistry*
*The Institute of Scientific and Industrial Research (SANKEN)*
*Osaka University*
*8-1 Mihogaoka, Ibaraki 567-0047 (Japan)*
*Fax: (+81) 6-6879-8459*
*E-mail: nakatani@sanken.osaka-u.ac.jp*

*Supporting information for this article is available on the WWW under http://www.chembiochem.org or from the author.*

  

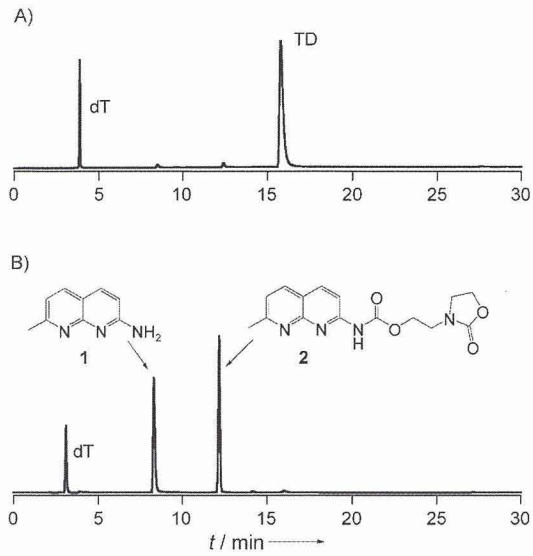


**Figure 1.** HPLC profiles for the thermolysis of TD (0.71 mM) in sodium cacodylate buffer (10 mM, pH 7.0). A) Before, and B) after heating at 80 °C for 4 min; deoxythymidine (dT) was added as an internal standard. After heating, TD underwent irreversible thermal fragmentation to form products **1** and **2**.

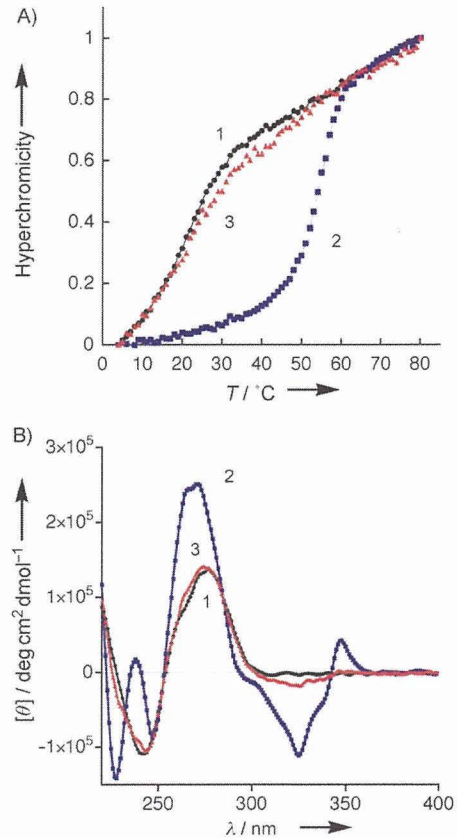


**Figure 2.** TD-assisted hybridization and denaturation. A) Thermal UV-melting curves were measured for duplex 5′-d(CCTTTGGTCAG)-3′/5′-d(CTGACGGAAGG)-3′ (4.5 μM) in sodium cacodylate buffer (10 mM, pH 7.0) containing NaCl (0.1 M). The temperature was increased from 4 to 80 °C at a rate of 1 °C min$^{-1}$. Sample 1: DNA only (●, $T_m$ = 21 °C); sample 2: DNA with TD (100 μM; ■, $T_m$ = 54 °C); sample 3: DNA with TD (100 μM) after being heated at 80 °C for 5 min and then gradually cooled to room temperature (▲, $T_m$ = 21 °C). B) CD spectra of the same samples used for melting curve measurements.

this is comparable with results obtained for the previous version of the molecular glue.[17] Since the cytosines in the CGG/CGG duplex are expected to be flipped out of the helix[18,20] (Scheme 1 B) they can be substituted with other bases in order to either decrease or increase the $T_m$ of the oligonucleotides.[17] Indeed, the $\Delta T_m$ value reached more than 30 °C ($T_m$ = 54.0 °C) for the 11-mer duplex 5′-d(CCTTTGGTCAG)-3′/5′-d(CTGACGGAAGG)-3′, which includes two contiguous T–G and G–G mismatches (Figure 2 A). TD markedly stabilized the mismatch-containing duplex, and apparently acted as molecular glue for DNA at room temperature. The function of TD, however, could be completely terminated by simple heating. After heating the TD-bound TGG/CGG mismatch-containing duplex at 80 °C for 5 min the $T_m$ value decreased back to the original value for this molecule (Figure 2 A). The marked change in duplex stability can be rationalized by quantitative and irreversible transformation of TD into the inactive form by heating. The transition between ssDNA and TD-bound dsDNA was clearly observed in the CD spectra (Figure 2 B). In the presence of TD, the CD spectrum of TGG/CGG mismatch-containing oligonucleotide was significantly different from the sample without TD. After heating the TD-containing sample at 80 °C for 5 min and subsequent gradual cooling to room temperature, its CD spectrum was virtually identical to that of the sample that did not contain TD.

DNA-functionalized gold nanoparticles have been intensively used for many applications, including the construction of nanostructures, biosensor, and diagnostic tools.[4,21] Reversible assembly/disassembly of gold nanoparticles has been achieved by the use of DNA or protons as fuel.[22,23] The transformation between ssDNA and TD-bound dsDNA shown above, was used to control the assembly of gold nanoparticles. Gold nanoparticles 15 nm in diameter were functionalized with DNA through a 5′-thiol-modified $A_{20}$ spacer, and two sets of DNA-modified gold nanoparticles, NP1 and NP2, were prepared (Figure 3 A).[21] The DNA sequences attached to NP1 and NP2 were hybridized with the linker DNA oligonucleotides L1 and L2, respectively. This resulted in the 5′-heptamer overhangs 5′-TTCGGTT-3′ and 5′-AATGGAA-3′ on L1 and L2, respectively. These overhangs contained the TD-binding site CGG/TGG. In the absence of TD, formation of the L1–L2 duplex by hybridization was not favored due to two contiguous T–G and G–G mismatches. As a result, the gold nanoparticles, NP1 and NP2, were dispersed in solution and therefore exhibited a red color due to plasmon absorption (Figure 3 B, state 1). In the presence of TD, plasmon absorption was red-shifted from 522 to 532 nm and the intensity decreased; this indicated the aggregation of the gold nanoparticles (Figure 3 B and C, state 2).[4,21–23] The molecular glue, TD, brought the overhang sequences in L1 and L2 together to form the TD-bound L1–L2 duplex, and assembled the NP1 and NP2 nanoparticles attached to the dsDNA. The aggregation of NP1 and NP2 particles was therefore propagated by their being coated with multiple DNA molecules. In

  

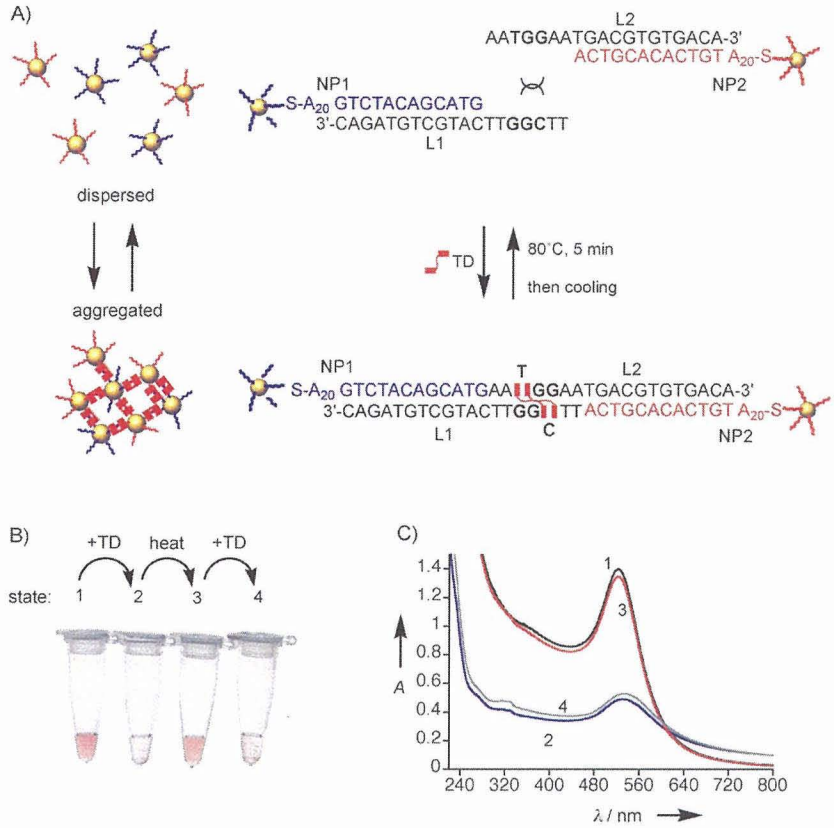


**Figure 3.** Control of gold nanoparticle assembly by using TD-assisted hybridization and denaturation. A) Illustration of nanoparticle assembly: the 5′-overhang heptamers on L1 and L2 contained the TD-binding CGG/TGG sequence (bold). Upon binding of TD to this sequence, the gold nanoparticles, NP1 and NP2, were assembled. After being heated at 80 °C for 5 min, TD was inactivated; this led to the disassembly of NP1 and NP2 aggregates. B) Colorimetric assay for nanoparticle aggregation in response to the function of TD: state 1, NP1 + NP2 + L1 + L2; state 2, NP1 + NP2 + L1 + L2 + TD; state 3, after heating state 2 solution at 80 °C for 5 min and gradual cooling to room temperature; state 4, TD + state 3 solution. C) UV-visible spectra of solutions of states 1–4.

marked contrast to the assembly of gold nanoparticles by using conventional DNA hybridization, particles aggregated through TD-binding could again be dispersed simply by heating the solution at 80 °C for 5 min (Figure 3B, state 3). The red color of the solution persisted at room temperature. This clearly indicates that heating caused inactivation of TD and conversion of the TD-bound L1–L2 duplex to single strands, and therefore the dispersion of NP1 and NP2. Upon addition of TD to the redispersed particles, aggregation took place again (Figure 3B, state 4). The changes in the plasmon absorption band from state 1 through to state 4 were monitored by UV-visible spectra, and were fully consistent with the assembly of gold nanoparticles in response to TD-assisted hybridization and denaturation of L1 and L2 (Figure 3C).

In summary, we have developed a new DNA molecular glue, TD, which allows bidirectional control of hybridization of unmodified DNA. This was demonstrated by the assembly and disassembly of gold nanoparticles. Bidirectional control of DNA hybridization will be applicable to DNA-based construction of nanostructures and -machines. Control of DNA hybridization by a small molecule provides a new strategy for constructing programmable DNA-based nanomaterials.

## Acknowledgements

*This work was supported by Grant in Aid for Scientific Research (S) from the Japan Society for the Promotion of Science.*

**Keywords:** DNA · gold · hybridization · mismatches · nanoparticles

[1] N. C. Seeman, *Nature* **2003**, *421*, 427–431.
[2] J. G. Hacia, *Nat. Genet.* **1999**, *21*, 42–47.
[3] Y. Ito, E. Fukusaki, *J. Mol. Catal. B Enzym.* **2004**, *28*, 155–166.
[4] N. L. Rosi, C. A. Mirkin, *Chem. Rev.* **2005**, *105*, 1547–1562.
[5] E. Katz, I. Willner, *Angew. Chem.* **2004**, *116*, 6166–6235; *Angew. Chem. Int. Ed.* **2004**, *43*, 6042–6108.
[6] U. Feldkamp, C. M. Niemeyer, *Angew. Chem.* **2006**, *118*, 1888–1910; *Angew. Chem. Int. Ed.* **2006**, *45*, 1856–1876.
[7] Z. Deng, S.-H. Lee, C. Mao, *J. Nanosci. Nanotechnol.* **2005**, *5*, 1954–1963.
[8] K. V. Gothelf, T. H. LaBean, *Org. Biomol. Chem.* **2005**, *3*, 4023–4037.
[9] B. Yurke, A. J. Turberfield, A. P. Mills, Jr., F. C. Simmel, J. E. Neumann, *Nature* **2000**, *406*, 605–608.
[10] H. Yan, X. Zhang, Z. Shen, N. C. Seeman, *Nature* **2002**, *415*, 62–65.
[11] J. S. Shin, N. A. Pierce, *J. Am. Chem. Soc.* **2004**, *126*, 10834–10835.
[12] H. Asanuma, T. Ito, T. Yoshida, X. Liang, M. Komiyama, *Angew. Chem.* **1999**, *111*, 2547–2549; *Angew. Chem. Int. Ed.* **1999**, *38*, 2393–2395.
[13] H. Asanuma, X. Liang, T. Yoshida, M. Komiyama, *ChemBioChem* **2001**, *2*, 39–44.
[14] B. Ghosn, F. R. Haselton, K. R. Gee, W. T. Monroe, *Photochem. Photobiol.* **2005**, *81*, 953–959.
[15] K. Hamad-Schifferli, J. J. Schwartz, A. T. Santos, S. G. Zhang, J. M. Jacobson, *Nature* **2002**, *415*, 152–155.
[16] J. Yang, J. Y. Lee, H.-P. Too, G.-M. Chow, *Biophys. Chem.* **2006**, *120*, 87–95.
[17] T. Peng, C. Dohno, K. Nakatani, *Angew. Chem.* **2006**, *118*, 5751–5754; *Angew. Chem. Int. Ed.* **2006**, *45*, 5623–5623.
[18] T. Peng, K. Nakatani, *Angew. Chem.* **2005**, *117*, 7446–7449; *Angew. Chem. Int. Ed.* **2005**, *44*, 7280–7283.
[19] T. Peng, T. Murase, Y. Goto, A. Kobori, K. Nakatani, *Bioorg. Med. Chem. Lett.* **2005**, *15*, 259–262.
[20] K. Nakatani, S. Hagihara, Y. Goto, A. Kobori, M. Hagihara, G. Hayashi, M. Kyo, M. Nomura, M. Mishima, C. Kojima, *Nat. Chem. Biol.* **2005**, *1*, 39–43.
[21] J. J. Storhoff, R. Elghanian, R. C. Mucic, C. A. Mirkin, R. L. Letsinger, *J. Am. Chem. Soc.* **1998**, *120*, 1959–1964.
[22] P. Hazarika, B. Ceyhan, C. M. Niemeyer, *Angew. Chem.* **2004**, *116*, 6631–6633; *Angew. Chem. Int. Ed.* **2004**, *43*, 6469–6471.
[23] Y. H. Jung, K.-B. Lee, Y.-G. Kim, I. S. Choi, *Angew. Chem.* **2006**, *118*, 6106–6109; *Angew. Chem. Int. Ed.* **2006**, *45*, 5960–5963.

Received: January 4, 2007
Published online on February 15, 2007

  

DOI: 10.1002/chem.200601496

# Allele Specific C-Bulge Probes with One Unique Fluorescent Molecule Discriminate the Single Nucleotide Polymorphism in DNA

**Fumie Takei,[a] Hitoshi Suda,[b] Masaki Hagihara,[a] Jinhua Zhang,[a] Akio Kobori,[b] and Kazuhiko Nakatani*[a, b]**

**Abstract:** A combination of an allele specific C-bulge probe and the fluorescent molecule *N,N'*-bis(3-aminopropyl)-2,7-diamino-1,8-naphthyridine (DANP) that binds specifically to the C-bulge provides a method for single nucleotide polymorphism (SNP) typing with only one fluorescent molecule without covalent modification of the DNA probe. The allele specific C-bulge probe contains one additional cytosine and produces a C-bulge directly flanking the SNP site upon hybridization to the target DNA. The C-bulge is a scaffold to recruit and retain DANP directly neighboring the SNP site. The DANP fluorescent probe was selectively modulated by the flanking matched and mismatched base pairs. The mutation type could be discriminated by the modulated fluorescent intensity with respect to the allele specific C-bulge probes used for the assay.

**Keywords:** cytosine bulge · DNA recognition · fluorescent probes · mutation detection

## Introduction

Typing of the single nucleotide polymorphisms (SNPs) in an individual genome against sets of predetermined disease-related SNPs is essential to achieve personalized medicine.[1–6] Besides methods which exploit the sequence-specific reactions of enzymes,[1–4] the challenge toward novel SNP typing methods based on organic chemistry draws attention to molecular systems that emit fluorescence in an allele specific manner.[7–19] Base discrimination by fluorescent molecules largely relies on the change in the fluorescent intensity upon formation of the matched or mismatched base pair. The chemical basis of the fluorescence change is a result of the modulation of the dielectric and hydrogen-bonding environments of the fluorescent chromophore. To exert the maximum influence of the base pairing on the fluorescence intensity, the fluorescent molecules have thus been developed near the SNP site by covalently linking the probe DNA and/or directly bind to the base at the SNP site.[7,15–19] In the latter strategy, the use of four fluorescent molecules selectively responding to each one of the four nucleotide bases has been investigated.[15–19]

In terms of convenience and simplicity of the assay, typing methods using fluorescent molecules would be particularly effective if the covalent modification of the probe DNA were not required, and if all four nucleotide bases could be analyzed by one unique fluorescent molecule. To address these issues, we have investigated a method exploiting allele specific C-bulge probe DNA and a fluorescent molecule selectively binding to the C-bulge. The C-bulge probe DNA is allele specific by alternating the nucleotide base ($^{Y}$N) opposite the SNP site ($^{X}$N) and contains one additional cytosine directly neighboring $^{Y}$N. The probe DNA provides a C-bulge as a scaffold to recruit and keep the fluorescent molecule directly neighboring the SNP site (Figure 1). We have reported that *N,N'*-bis(3-aminopropyl)-2,7-diamino-1,8-naphthyridine (DANP) selectively and strongly bound to the C-bulge with an exclusive 1:1 stoichiometry.[20] DANP binds to the C-bulge as the protonated form DANPH$^+$ at a neutral pH (Figure 2). Therefore, DANP would be recruited to the cytosine bulge that is located directly adjacent to the matched or mismatched base pair $^{X}$N–$^{Y}$N at the SNP site. DANPH$^+$ emitted characteristic fluorescence upon binding to the cytosine bulge. Upon binding, both absorption and emission maximum of DANPH$^+$ were shifted by 30 nm to a longer wavelength from those of the unbound DANP. Therefore, it is possible to selectively monitor the DANPH$^+$

[a] Dr. F. Takei, Dr. M. Hagihara, Dr. J. Zhang, Prof. K. Nakatani
Department of Regulatory Bioorganic Chemistry
The Institute of Scientific and Industrial Research
Osaka University, 8-1 Mihogaoka, Ibaraki 567-0047 (Japan)
Fax: (+81) 6-6879-8459
E-mail: nakatani@sanken.osaka-u.ac.jp

[b] H. Suda, Dr. A. Kobori, Prof. K. Nakatani
Department Synthetic Chemistry and Biological Chemistry
Kyoto University, Nishigyou-ku, Kyoto 615-8510 (Japan)

   